

Identifying the source of tar balls deposited along the beaches of Goa in 2013 and comparing with historical data collected along the West Coast of India

V. Suneel¹, P. Vethamony^{1*}, B. G. Naik¹, M. S. Krishna², Lakshmikant Jadhav¹

¹CSIR-National Institute of Oceanography, Dona Paula, Goa 403004, India

Email ID: vasimallas@nio.org; mony@nio.org; bgnaik@nio.org; lakshya87.0@gmail.com

² CSIR-National Institute of Oceanography, Regional Centre, Visakhapatnam-530 017

India. Email id: moturi@nio.org

***Corresponding author: P. Vethamony**, CSIR-National Institute of Oceanography, Dona Paula, Goa 403004, India. Email: mony@nio.org, Tel +91 832 2450473; Fax No. +91 832 2450608

Abstract

Deposition of oil residues, also known as tar balls, is a seasonal phenomenon, and it occurs only in the southwest monsoon season along the west coast of India. This has become a serious environmental issue, as Goa is a global tourist destination. The present work aims at identifying the source oil of the tar balls that consistently depositing along the Goa coast using multi-marker fingerprint technique. In this context, the tar ball samples collected in May 2013 from 9 beaches of Goa coast and crude oils from different oil fields and grounded ship were subject to multi-marker analyses such as n-alkanes, pentacyclic terpanes, regular steranes, compound specific isotope analysis (CSIA) and principle component analysis (PCA). The n-alkane weathering index shows that samples have been weathered to various degrees, and the status of weathering is moderate. Since the international tanker route passes closer to the west coast of India (WCI), it is generally presumed that tanker wash is the source of the tar balls. We found that 2010/2011 tar balls are as tanker wash, but the present study demonstrates that the Bombay High (BH) oil fields can also contribute to oil contamination (tar balls) along ≈ 650 km stretch of the WCI, running from Gujarat in the north to Goa in the south. The simulated trajectories show that all the particles released in April travelled in the southeast direction, and by May, they reached the Goa coast with the influence of circulation of Indian monsoon system.

Key words: tar balls, oil spill, Bombay High, fingerprinting, terpanes, steranes, isotopes

1. Introduction

Deposition of oil residues on the coast in the form of tar balls has become a serious issue along the central and northern parts of the west coast of India (WCI) in which the Goa coast is consistently got affected by the tar ball deposition every year. Though this problem was noticed as early as 1970, very few studies (Nair et al. 1972, Dwivedi and Parulekar, 1974, Dhargalkar et al. 1976, Sengupta and Kureishy, 1981, Kadam, 1988) were carried out to understand the chemical characteristics of the tar balls. Suneel et al. (2013a) have analyzed the tar balls that deposited during 2010 and 2011 along the Goa coast and found that they were derived from tanker-wash. This is understandable as Goa is located in the centre of the WCI and the tanker route passes very closer to the coast. However, the tanker-washes were strictly prohibited since 2011. Since August 2010, we have been monitoring tar ball deposition activities and analyzing their chemical characteristics and fingerprints. The monitoring reveals that the deposition is consistent along the coastal stretch between the central WCI and the northern WCI.

The analysis of tar ball samples deposited along the Gujarat coast in July 2012 showed that they were derived from the BH oil fields (Suneel et al. 2014). It may be noted that tanker wash is not the only source until 2010, and BH is the source after 2010; tar balls might have been formed by the BH oil fields even before 2010, but we have not collected and analyzed until 2010. No deposition has occurred on the southern part of the WCI in the last 4 years, except the one in June 2014 along the Majali coast near Karwar (Karnataka). Thus, this is high time to find out the source of the tar balls along the WCI, especially the Goa coast as the Goa beaches attract global tourism. Tar ball deposition affects tourism, which in turn bring down the economy of Goa. In this context, we initiated this work to investigate whether tanker wash alone is the source of tar balls deposited along the Goa coast or Bombay High, Cairn and Niko oil fields could also be the sources. The study area and the locations of tar ball deposition along the Goa coast are presented in Fig. 1.

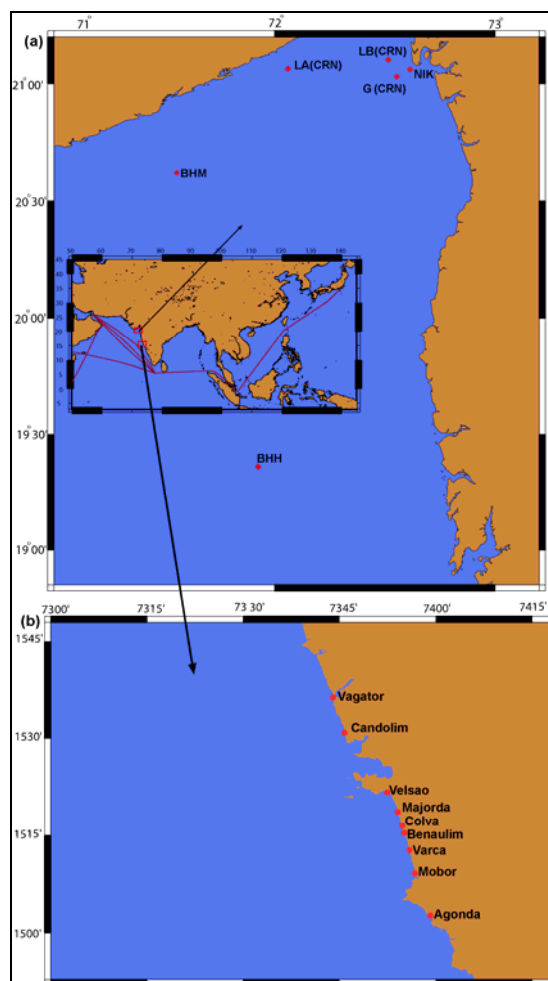


Fig. 1. The sampling locations: (a) locations of oil fields and (b) tar ball sampling locations. The distance between a & b is ≈ 600 km

Winds, surface currents and tides are the major forces that deliver tar balls to the WCI during pre-monsoon and monsoon seasons; southwest monsoon is the conducive period for the deposition of tar balls along the WCI (Suneel et al. 2013 a, b). The possible spill sources in the Arabian Sea (AS) are (i) Offshore oil fields located off Mumbai-Gujarat coast, (ii) Tanker washes if any, along the International tanker route which connects the Persian Gulf to the far eastern countries (iii) Discharge through the refineries, industries, power plants, minor and major ports located offshore of the Gujarat. (iv) oil spills due to tanker accidents (Suneel et al. 2014). The Bombay High (BH) oil fields located 162 km west-northwest of Mumbai, in a water depth of 75 m, and a few of the wells are shown in Fig. 1a.

Various fingerprint techniques have been developed and applied to anonymous spills/ tar balls deposited along the coastal stretches (Kvenvolden et al. 1995, Page et al. 1995, Boehm et al. 1997,

Wang et al. 1995a, 1997, 2001a, and 2004). However, in order to make more reliable and defensible correlations, the use of a “multi-criteria approach” is often a pre-requisite. In a multi-criteria approach, the conclusion is based on analysis and evaluation of distribution of more than one suite of petroleum compounds (Wang et al. 1999a; Stout et al. 2002; Daling et al. 2002; Christensen et al. 2004; Peters et al. 2005). CSIA is widely used in marine environmental studies primarily to track the sources, and perform the correlation between oils and their source rocks. The isotope ratios of individual hydrocarbons are generated during the formation of the organic matter (plant photosynthesis), subsequent to petrogenesis and refinery processes (Meckenstock et al. 2004). Therefore, each type of oil will have a unique isotope signature; consequently, even if the concentrations of individual components change over time, the isotope ratios of the individual components may remain the same. These ratios depend on the depositional environment, type of kerogen, migration pathways, type of oil and the age of the source rocks (Galimov, 1973). They can be used to establish a genetic relationship between a number of oil types (Rabbani and Galimov, 2000; Galimov and Rabbani, 2001; Rabbani and Kamali, 2005). Weathering, water-washing and evaporation cannot alter the isotope ratios (Jeffrey, 2006), for example, Macko et al. (1981) observed only 0.5‰ difference in the $\delta^{13}\text{C}$ values after 2 years of weathering.

The short term weathering processes such as evaporation and dispersion cannot affect the carbon isotope composition ($\delta^{13}\text{C}$) values of individual n-alkanes (Mansuy et al. 1997; Li et al. 2009). Though, weathering causes loss of volatile compounds, $\delta^{13}\text{C}$ values of non-volatile and semi-volatile compounds are unaffected by weathering and their isotopic ratios can be used to trace the oil spill source (Betti et al. 2011). Stable isotopes are resistant to decay over geological time scales and widely used for source identification and fingerprinting (Oulhote et al. 2011). Fingerprinting of unknown oil spills and tar balls is possible by Gas Chromatographic techniques such as GC-FID and GC-MS. CSIA is an additional technique to fingerprint the spill or tar balls in more persistent cases. Many researchers have used this technique to identify the sources and characterize the crude oils (Macko et al. 1983; Murray et al. 1994; Kvenvolden et al. 1993, 1995; Mansuy et al. 1997; Wang et al. 1998). In the present study, CSIA analysis was performed on all the 18 tar ball and 5 crude oil samples. The homologue series of regular steranes $5\alpha(\text{H}),14\beta(\text{H}),17\beta(\text{H})$ Cholestane (C_{27}), $5\alpha(\text{H}),14\beta(\text{H}),17\beta(\text{H})$ Ergostane (C_{28}) and $5\alpha(\text{H}),14\beta(\text{H}),17\beta(\text{H})$ Stigmastane (C_{29}) are the most useful compounds for chemical fingerprinting. The sterane compounds C_{27} , C_{28} and C_{29} are usually withdrawn by the types of photosynthetic organisms which contribute to the organic matter that are useful in determination of petroleum origin, depositional environment and relationship between oil and source rock (Peters and Moldowan, 1993). The C_{27} steranes are abundant and dominant in marine

organic matter, but the C₂₈ steranes are originated from the marine phytoplankton and lake algal and C₂₉ steranes dominate in terrigenous organic matter (Grantham and Wakefield, 1988).

In the present study, the samples collected from various beaches of Goa (18 tar balls) and 5 probable source crude oils [Bombay High Mut (BHM_{oil}), Bombay High Hut (BHH_{oil}), Cairn oil fields (CRN_{oil}), Niko oil fields (NIK_{oil}) and MSC Chitra tanker spill (MSC_{oil})] were analyzed by multifarious class of compounds such as n-alkanes, pentacyclic terpanes (hopanes), regular steranes (C₂₇, C₂₈, C₂₉) and their source specific Diagnostic Ratios (DRs). Compound Specific Isotope Analysis (CSIA) and principle component analysis (PCA) were also carried out to confirm the source of the tar balls (Betti et al. 2011, Oulhote et al. 2011, Christensen et al. 2004, and Li et al. 2004).

2. Materials and methods

The concentrations of the targeted compounds were determined in µg/gm of sample. For example, we have calculated the concentration of C₂₉ and C₃₀ hopanes in µg/gm of tar ball/oil and calculated the diagnostic ratio C₂₉/C₃₀. Similarly, we have calculated for all alkane and hopane diagnostic ratios. L/H is defined based on the molecular weight of the normal alkane components. The ratio of sum of low molecular weight n-alkanes (n-C₁₆ to n-C₂₆) relative to high molecular weight n-alkanes (n-C₂₇ to n-C₃₆); L/H= $\sum(n-C_{16} \text{ to } n-C_{26}) / \sum(n-C_{27} \text{ to } n-C_{36})$ (Zakaria et al. 2001). Wang and Fingas (1994) developed the weathering index (WI) by using n-alkanes such as C₈, C₁₀, C₁₂, C₁₄ and C₂₂, C₂₄, C₂₆, C₂₈. Therefore,

$$\text{Weathering Index} = \left(\frac{C_8 + C_{10} + C_{12} + C_{14}}{C_{22} + C_{24} + C_{26} + C_{28}} \right)$$

The most commonly used diagnostic ratios (DRs) for the alkanes are Pr/Py; n-C₁₇/Pr; n- C₁₈/Ph, n-C₁₇/n-C₁₈, CPI, Light/Heavy (L/H) and Weathering Index (WI). These ratios decrease only during initial phase of weathering. The isoprenoid alkanes such as pristane and phytane are more resistant to degradation (Barakat et al. 2002), whereas n-C₁₇ and n-C₁₈ can vanish rapidly compared to isoprenoid alkanes ensuing that the ratios n-C₁₇/Pr and n-C₁₈/Py decrease in weathered samples. Therefore, n-C₁₇/Pr and n-C₁₈/Py indices have been widely used as indicators of oil biodegradation (Barakat et al. 2001; Wang and Fingas, 2003). Biomarkers such as pentacyclic terpanes and regular steranes have the distinctive property of being greatly resistant to weathering, and therefore, they have been widely used in oil spill forensic studies (Wang et al. 1994b; 1995b; Zakaria et al. 2000, 2001; Chandru et al. 2008). According to the genesis of crude oil in different geological time scales, a unique biomarker fingerprint will form, and thus, biomarker analysis plays a prominent role in fingerprinting of tar

balls. In the present study, the DRs of pentacyclic terpanes C_{29}/C_{30} , $\sum C_{31}-C_{35}/C_{30}$, Tm/C_{30} , $Oleanane/C_{30}$, Ts/Tm , $C_{31}S/(S+R)$, $C_{32}S/(S+R)$, $C_{33}S/(S+R)$, $C_{34}S/(S+R)$ and $C_{35}S/(S+R)$ of tar balls are calculated, and compared with the ratios of crude oils. We have listed out all the acronyms that are used in this paper in Table. SM1.

2.1. Sample collection

Tar ball samples (18 Nos.) were collected from 9 beaches of the Goa coast (Table. SM2) using stainless steel spatula placed in labeled glass bottles and stored in the laboratory refrigerator ($-20^{\circ}C$). The physical properties of collected tar balls are dark brown/mud stone in color, solid form with hard surface but soft core, mixed with sand particles. Though we have used 130 mg of tar ball samples from each sample, the entire mass of tar balls varies, as per the sizes. We have weighed a few samples: the mass of tar balls ranges from $\approx 1.8g$ to $47g$ and the size ranging from $\approx 1cm$ to $7cm$. In order to understand whether the collected tar balls were floating or suspended in the water column, an experiment was done in the laboratory, by dropping each tar ball into the beaker of sea water having a salinity of 33.7 psu and temperature of $26.9^{\circ}C$, and we observed that all the tar balls were floating at the surface. The distance between the sample collection sites are given as indicated in Fig. 1b. The distance between Vagator and Candolim is ≈ 10 km; Candolim and Velsao is ≈ 20 km; Velsao and Majorda ≈ 5 km; Majorda and Colva ≈ 4 km; Colva and Benaulim ≈ 3 km; Benaulim and Varca ≈ 2.5 km; Varca and Mobor ≈ 8 km; Mobor and Agonda ≈ 20 km. The fingerprinting results of BHM_{oil} , BHH_{oil} , CRN_{oil} , NIK_{oil} and MSC_{oil} were taken from the earlier study (Suneel et al. 2014) in order to compare with the results of present tar ball samples. Fig. 1 shows the sampling locations and the international tanker route connecting the Arabian Gulf to Japan through the AS. A typical example for tar ball deposition on the Mobor beach of Goa in May 2013 is shown in Fig. SM1, (Supplementary Material).

2.2. Chemicals, Extraction, fractionation and analysis

Authentic standards for n-alkanes (Sigma Aldrich, USA), hopanes $17\beta(H)$ $21\alpha(H)$ -hopane ($C_{30}17\beta\alpha$) and $17\alpha(H)$ - 22, 29, 30- trisnorhopane (Tm) (Chiron, Norway) were used as a reference standards to identify the n-alkane, hopane compounds. A silica gel with mesh 60-120 was baked at $400^{\circ}C$ for 4 h, cooled, then activated at $200^{\circ}C$ overnight and deactivated with 5% of distilled water. Organic solvents were distilled in glass before use to purify the solvents, which will be useful for obtaining better accuracy in the chromatography. All glassware were washed with detergents, tap water, and then rinsed with methanol, acetone and hexane.

Crude oil and tar ball samples were weighed precisely (130 mg) and dissolved in 50 ml of n-hexane. From this, 10 ml of solution (Equivalent to the 26mg of tar ball) was taken and transferred to 5% H₂O deactivated silica gel column (1cm i.d × 9cm). The core of the tar ball (not from the surface layer) was taken for the analysis, as the rate of weathering is slower than the outside area due to lack of oxygen and microbial mineralization and therefore more suitable for source identification. Detailed analytical processes and fractionations are given in Suneel et al., (2014). Analyses for *n*-alkane, steranes and hopanes were performed using a Shimadzu QP-2010 gas chromatograph and mass spectrometer, interfaced with an AOC-20i auto sampler. Carbon isotopic ratios of individual *n*-alkanes were determined on Isoprime100 IRMS, coupled with Agilent 7890A GC-MS and interfaced with oxidation-reduction reactor (980-650°C). The description of GC-MS and GC-IRMS and their performance check, quality control and quality assurance are given in Suneel et al (2014). Identification procedure for sterane compounds is described in section SM. 1, Supplementary Material, and the sterane chromatograms for one tar ball sample and one crude oil are given in Fig. SM2, Supplementary Material. PCA is a multivariate statistical tool that is widely used in the interpretive of oil spill fingerprinting. The PCA transforms the data into principal components. Samples of similar chemical compositions were clustered together, and samples which are chemically different were separated, and this helps in source identification.

3. Results and Discussion

3.1. Distribution of hydrocarbons and weathering

Petroleum and its products contain a range of hydrocarbons, in which the alkanes are often used for the estimation of degree of weathering. The carbon preference index (CPI) is calculated using the *n*-alkanes and the value of CPI is normally 1.0 for petroleum products. In the present study, CPI values of all tar ball samples varied between 1.09 and 1.10, confirming that the tar balls had originated from petroleum. The calculated DRs in the present study are lower than those of crude oils (Table SM3). The weathering Index (WI) values reveal that samples have been weathered to various degrees, ranging from 0.01 to 0.08 indicating moderate weathering, except for the samples MOB-1_{tb} and VEL-2_{tb}, for which the values are very low (0.004, 0.002) signifying that they have weathered severely. The L/H ratio of tar balls is also less compared to the crude oils, suggesting that the samples had weathered significantly (might be due to biodegradation). We observed that the compound phytane was less abundant in all crude oils except MSC, resulting in higher ratios of Pr/Py and *n*-C₁₈/Py; the same feature is noticed in all tar ball samples; moreover, these DR values are very near to the DR values of BHM_{oil} compared to the other crude oils (Table SM2). Though the core of the tar

ball has been taken for analysis, the n-alkane analysis illustrates weathering in all tar ball samples. This observed weathering might have taken place during transition period between the oil spill (might be minor, but continuous) and the tar ball formation. The core of the tar ball can only slowed down the weathering after tar ball formation is complete. The ratio Pr/Py clearly differentiated the tar balls and crude oils, and match closely only with the BHM crude (Table SM3). The same DR also has shown significant difference between BHM_{oil} and BHH_{oil} characteristics (4.99 and 6.03, respectively). Based on the DRs (L/H and WI), we can say that the tar ball samples have been weathered to different degrees. The ratios of MSC were completely different ratios than of tar balls. Therefore, based on the DRs- Pr/Py, C₁₇/Pr, C₁₈/Py, we can say that the tar balls have been biodegraded considerably and the source might be BHM_{oil}

3.2. Source specific biomarker fingerprints

The chromatographs obtained for hopanes using m/z-191 were practically identical for all the tar ball samples (Fig. 2). Visual comparison of these chromatograms with the crude oil chromatograms (Fig. 3) suggests that tar balls meticulously resemble the BHM_{oil} chromatograms. A close observation shows that MSC_{oil} crude is enriched in C₂₉, whereas the remaining crude oils are abundant in C₃₀. The tar ball samples are also enriched in C₃₀ (Fig. 2), confirming that MSC_{oil} is not the source. Moreover, the compound Oleanane normally presents in the crude oil, formed due to plant material deposition in the deltaic environment (Sosrowidjojo et al. 1994). This particular property is helpful in identifying the source of anonymous oil spills. The Oleanane is absent in MSC_{oil}, but present in the CRN_{oil}, NIK_{oil}, BHH_{oil} and BHM_{oil} samples. Among all crudes, the BHM is more enriched in Oleanane. Interestingly, all the tar balls are also enriched in oleanane. We have further examined the DRs of pentacyclic terpanes C₂₉/C₃₀ and $\sum C_{31}-C_{35}/C_{35}$ (homohopane index), which are reliable source identifiers in oil spill forensic studies (Zakaria et al., 2001, Suneel et. al., 2013a, Suneel et. al., 2014).

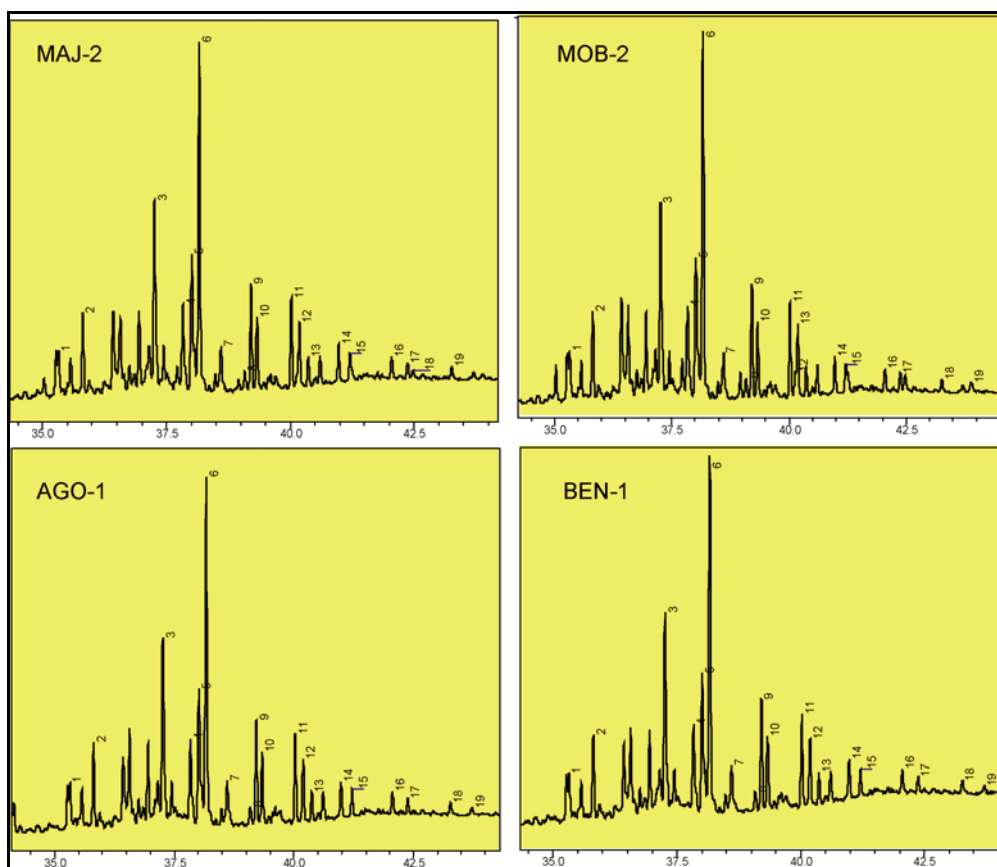


Fig. 2. GC-MS Hopane chromatograms (m/z-191) for the sample of Maj-2, MOB-2, AGO-1 and BEN-1. 1-Ts, 2-Tm, 3-C₂₉ α , 4-C₂₉ β , 5-OL, 6- C₃₀ $\alpha\beta$, 7- C₃₀ $\beta\alpha$, 8- C₃₁ $\alpha\beta$ -S, 9- C₃₁ $\beta\alpha$ -S, 10-C₃₁ $\alpha\beta$ -R, 11- C₃₂ $\alpha\beta$ -S, 12- C₃₂ $\beta\alpha$ -S, 13-C₃₂ $\alpha\beta$ -R, 14- C₃₃ $\alpha\beta$ -S, 15- C₃₃ $\alpha\beta$ -R, 16- C₃₄ $\alpha\beta$ -S, 17- C₃₄ $\alpha\beta$ -R, 18- C₃₅ $\alpha\beta$ -S, 19- C₃₅ $\alpha\beta$ -R.

The biplot between the ratios C_{29}/C_{30} and $\sum C_{31}-C_{35}/C_{35}$ has been made for the present tar ball samples by including the DRs of a few MECO and SEACO obtained from the published data (Zakaria et al. 2000) (Fig. 4). Fig. 4 clearly shows that the tar ball samples (blue diamonds) in black circle do not match with MECO (red circle), SEACO (pink circle), MSC_{oil} (green) or CRN_{oil} and NIK_{oil} (dark yellow), but precisely match with the BH crude oils (the pink diamonds in the black circle). The DRs such as Ts/Tm, Tm/C₃₀, Oleanane/C₃₀, C₃₁(22S)/C₃₁(22S+22R), C₃₂(22S)/C₃₂(22S+22R), C₃₃(22S)/C₃₃(22S+22R), C₃₄(22S)/C₃₄(22S + 22R), and C₃₅(22S)/ C₃₅(22S + 22R) used in recent studies (Mulabagal et al. 2013) have also been calculated in this present work.

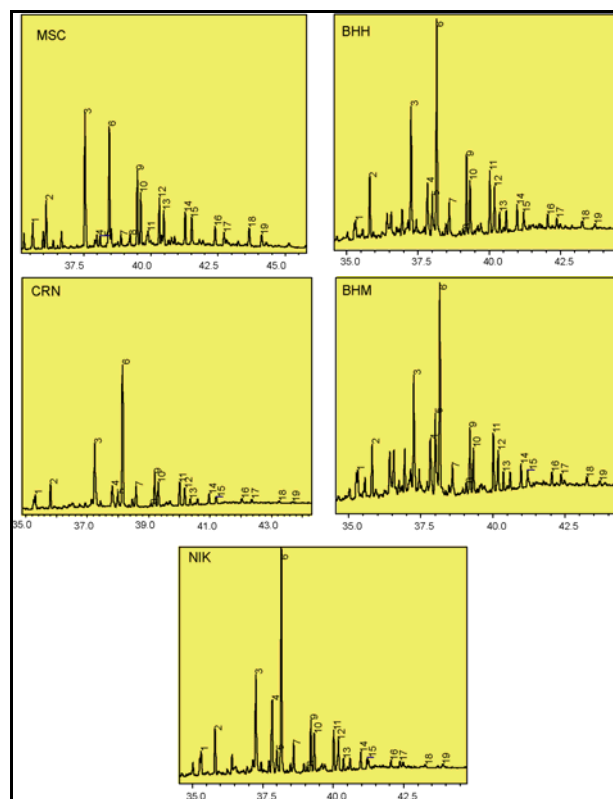


Fig. 3. GC-MS hopane chromatograms (m/z 191) for the crude oil samples. Peak numbers 1-19 show the hopane compounds as 1-Ts, 2-Tm, 3-C₂₉ α , 4-C₂₉ β , 5-OL, 6- C₃₀ $\alpha\beta$, 7- C₃₀ $\beta\alpha$, 8-C₃₁ $\alpha\beta$ -S, 9- C₃₁ $\beta\alpha$ -S, 10-C₃₁ $\alpha\beta$ -R, 11- C₃₂ $\alpha\beta$ -S, 12- C₃₂ $\beta\alpha$ -S, 13- C₃₂ $\alpha\beta$ -R, 14- C₃₃ $\alpha\beta$ -S, 15- C₃₃ $\alpha\beta$ -R, 16- C₃₄ $\alpha\beta$ -S, 17- C₃₄ $\alpha\beta$ -R, 18- C₃₅ $\alpha\beta$ -S, 19- C₃₅ $\alpha\beta$ -R

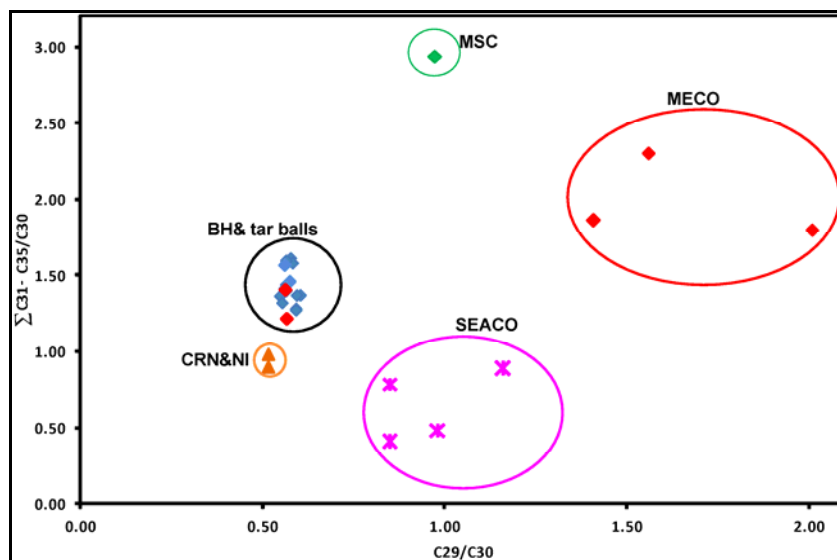


Fig. 4. Biplot between the ratios C₂₉/C₃₀ Vs $\sum C_{31}-C_{35}/C_{30}$ for tar balls crude oils. The red and diamonds in black circle are BH crude oils (BHM_{oil} & BHH_{oil}) and tar balls respectively, showing the match between tar balls and BH crude.

Referring to Table SM4, DR values of Tm/C₃₀ of tar balls vary from 0.20 to 0.22 except for the AGO-1_{tb} sample and match with BHM_{oil}. Similarly, the values of Ts/Tm and Oleanane/C₃₀ of all the samples also match with BHM_{oil}. In order to confirm that all the tar balls were derived from the same source, the variation in DRs of the samples is measured by calculating the standard deviation (S.D) of DRs. The S.Ds of C₃₁S/(S+R), C₃₂S/(S+R), C₃₃S/(S+R), C₃₄S/(S+R), and C₃₅S/(S+R) are 0.01, 0.02, 0.04, 0.15 and 0.20, respectively. Thus, the pentacyclic triterpanes and their DRs show that all the tar ball samples were derived from the same source, namely, BHM_{oil}.

All the crude oils and tar balls that we studied were enriched in C₂₇ steranes, revealing that all the source rocks were probably deposited in an open marine environment, supporting our argument that the source may be BH crude. The distribution of these regular sterane compounds of all tar ball samples and crude oils is illustrated in the ternary plot (Fig. 5). Fig. 5 distinctly brings out the relation between the samples (black triangles) and the crude oils (labeled). The MSC_{oil}, NIK_{oil} and CRN_{oil} crude characteristics are quite different from the tar balls, but, NIK_{oil} and CRN_{oil} have the same characteristics, probably, because CRN_{oil} and NIK_{oil} oil fields are closer to each other (hence, only NIK_{oil} is presented here). The hopane data also shows the same features (Fig. 3). However, significant differences in crude oil characteristics exist between BH_{oil} (C₂₇-70, C₂₈-30, C₂₉-63) and NIK_{oil} (C₂₇-83, C₂₈-16, C₂₉-84) crudes. The red and blue diamonds in Fig. 5, represent BHM_{oil} and BHH_{oil}, respectively and they fall in the midst of tar balls, confirming that the source is definitely BHM_{oil} crude oil.

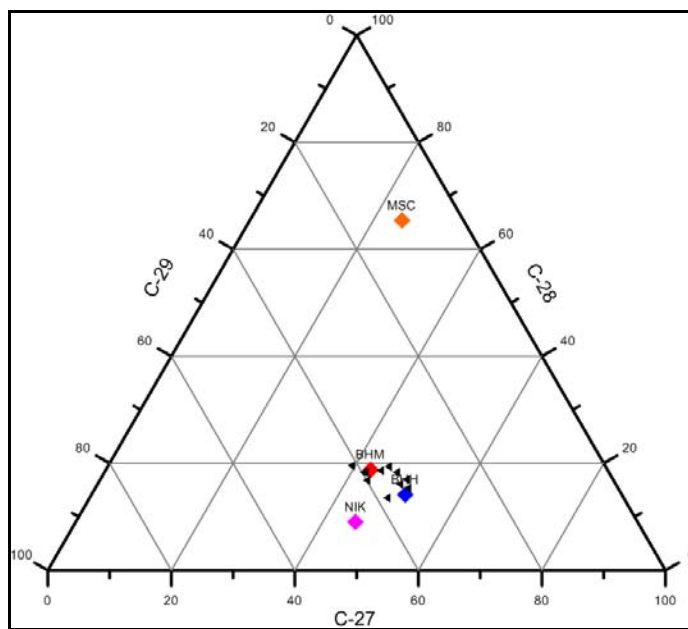


Fig. 5. Distribution of regular sterane compounds showing the relation between the crude oils and tar samples. The red, blue, pink and dark yellow diamonds represent BHM, BHH, NIK and MSC crude oils; black triangles show tar ball samples.

3.3. Compound Specific Isotope Analysis (CSIA)

The CSIA results show that n-alkane $\delta^{13}\text{C}$ ratio lines of BHM_{oil} and BHH_{oil} follow almost identical patterns; similarly, the CRN_{oil} and NIK_{oil} crudes also apparently follow the identical patterns (Fig. 6). This is because BHM_{oil} and BHH_{oil} are generated from the Bombay High basin fields, whereas, the CRN_{oil} and NIK_{oil} are generated offshore of Gujarat. However, there are significant differences between BH crude oils and CRN_{oil} and NIK_{oil} crude oils. The $\delta^{13}\text{C}$ ratios of lower molecular components (C_{15} - C_{26}) of BH crude oils are isotopically heavier than CRN_{oil} or NIK_{oil} crude oils, while higher molecular components (C_{26} - C_{35}) of BH, CRN_{oil} and NIK_{oil} are lighter, but closer to each other (Fig. 6). It is reverse in the case of MSC_{oil} crude. The $\delta^{13}\text{C}$ ratios of alkanes beyond C_{20} are isotopically heavier than tar balls, BH crude oils and CRN_{oil} and NIK_{oil} crude oils. Therefore, the MSC_{oil} , CRN_{oil} and NIK_{oil} crudes are not the sources for the tar ball samples. There exists a good match between BH crude oils and the tar ball samples; n-alkane $\delta^{13}\text{C}$ ratios follow the same pattern for both the crude oils (BHM_{oil} and BHH_{oil}) and all tar balls, thereby confirming that the source of tar balls is BH crude oil only.

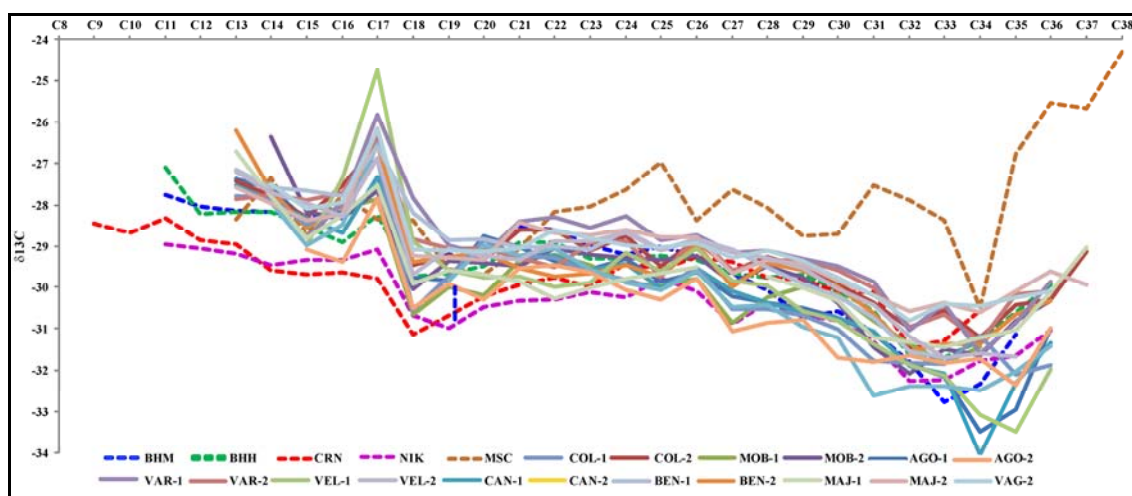


Fig. 6. Compound specific isotope analysis for tar balls and crude oils

3.4. Chemometric data analysis

PCA was done to contemplate the maximum amount of variation contained in the isotopic data sets and to confirm the source (Fig. 7). The MSC_{oil} , CRN_{oil} and NIK_{oil} apparently differ from the tar ball samples and BH crude oils. The variation for the first two principal components F1 and F2 accounts for about 90.9%. Though NIK_{oil} crude falls close to the tar balls, the BH oils are even more closer to the tar balls. This is another confirmation to state that tar ball samples were originated from the BH oil fields; to be specific, from BHM_{oil} only as illustrated by the DRs of alkane and hopane.

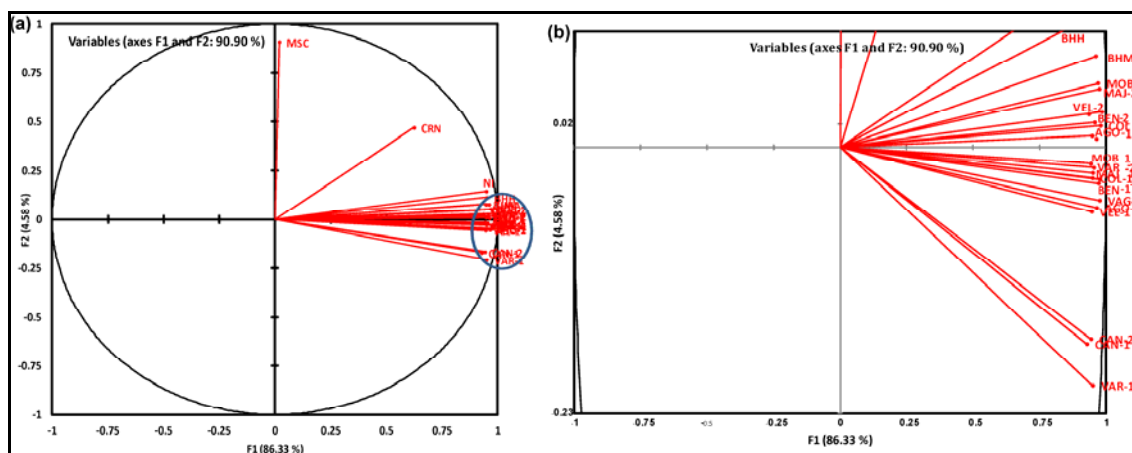


Fig. 7. (a) Variable axes for the first two principal components of PCA for the isotopic data and (b) the zoomed picture of circle drawn in Fig. 7a for the purpose of visualization.

In our earlier work (Suneel et al., 2013b, 2014), we found that the transport of tar balls to the WCI is primarily driven by the seasonal circulation of Arabian Sea, forced by winds, currents and tides. However, the hydrodynamic model coupled with particle tracking set up for the Goa coast revealed that tar balls deposited along the Goa coast during 2010 were due to tanker washes along the international tanker routes. The same has been confirmed in fingerprint analysis, which shows that tar balls were derived by the tanker washes (Suneel et al. 2013a). Whereas, the same model set up for the Gujarat coast reveals that the tar balls deposited during July 2012 along the Gujarat coast were derived from the BH oil fields (Suneel et al. 2014). Present study focused only on fingerprint analysis by using the reliable source specific biomarkers. The results show that 2013 tar balls off Goa are not from tanker wash, but from the BH oil fields. Now the question is, how were these tar balls transported to the Goa coast, which is ≈ 600 km from BH_{oil} fields (towards southeast)? This could be inferred from the the simulated tar ball trajectories presented in Suneel et al. (2014). Trajectories of the particles that were released near the BH_{oil} fields during April, May, June and July 2012 reached the Gujarat coast. However, a close look at the April simulation results show that all the particles travelled in the southeast direction (towards Goa coast), and by May, they reached the Goa coast (Fig. SM3, Supplementary Material). In general, this is the general circulation pattern presents every year due to Indian summer monsoon. The tar balls might have started from its original position in April, and arrived the Goa coast in May. However, detailed study is required to confirm this, and the work is in progress.

3. 5. Conclusion

In the present study, multi-criteria approach such as DRs of n-alkanes, cross-plots of pentacyclic terpanes, regular sterane compounds, CSIA and PCA were used for fingerprinting

the source of the tar balls deposited along the Goa coast during May 2013. The n-alkane DRs (even core of the tar balls) reveal that weathering might have occurred during the transition time from the oil spill to tar ball formation. The Pr/Py ratio of tar balls matches with the BHM_{oil} crude, but not with other crude oils. The DRs of hopanes and the cross plot between their DRs clearly illustrate the source as BH, especially BHM_{oil}. The sterane, CSIA and the PCA confirm that the source is Bombay High crude only. The n-alkane and hopane DRs show significant difference between crude oils, but matching with BHM_{oil}. The tar ball samples collected from the beaches of Goa during 2010/2011 were identified as those derived from the tanker washes. As tanker wash activities have been banned since 2011, the tar balls deposited before 2011 could have been a combination of both Bombay High and tanker washes, but no samples (before 2010) available to prove this and confirm. Based on the data presented in our current and previous studies (e.g., Suneel et al. 2014) we conclude that the 2013 tar balls should have originated from Bombay High crude. . The causes for the BH crude oil spill are not known - could be leakage in the pipelines, natural seepage or multiple causes, and this demands for long-term monitoring.

Acknowledgements

We thank the Director, Dr. S.W.A. Naqvi, CSIR-National Institute of Oceanography for his encouragement and support towards this work. Suneel is thankful to the CSIR for the Senior Research Fellowship. Thanks are due to Dr. Aninda Majumdar for providing wet lab and GCMS facilities. Sreenu is acknowledged for his help in isotope analysis. This is CSIR-NIO contribution number xxxx.

References

1. Nair, A, V. P. Devassy, S. N. Dwivedi, R. A. Selvakumar, 1972. Tar ball pollution in Central west coast of India. *Current Science* 41, 766-767.
2. Boehm, P. D., G. S. Douglas, W. A. Burns, P. J. Mankiewicz, D. S. PAGE and A. E. Benc. 1997 Application of Petroleum Hydrocarbon Chemical Fingerprinting and Allocation Techniques after the Exxon Valdez Oil Spill. *Marine Pollution Bulletin*, 34, 8, 599- 613.
3. Dwivedi, S. N and A. H. Parulekar, 1974. Oil pollution along the Indian coastline. NBS special publication. 409, *Marine Pollution Monitoring (petroleum)*, Proceedings of a symposium and workshop held at NBS, Galthersburg, Maryland, May 13-17.
4. Dhargalkar V. K, T.W. Kureishy and M.V. Bhandare, 1976. Deposition of tar balls (Oil residue) on beaches along the west coast of India. *Mahasagar: Bulletin of the National Institute of Oceanography*, 10 (3 & 4), 103-108.
5. Sengupta, R., T. W. Kureishy., 1981. Present state of oil pollution in the northern Indian Ocean *Marine Pollution Bulletin*, 12(9), 295-301.
6. Kadam, A. N, 1988. Some Studies on Tar pellets at Veraval Coast (Gujarat). *Mahasagar, Bulletin of National Institute of Oceanography*, 21, 173 -175.

7. Suneel, V., P. Vethamony., M. P. Zakaria., B. G. Naik., K. V. S. R. Prasad, 2013a. Identification of sources of tar balls deposited along the Goa coast, India, using fingerprinting techniques. *Mar. Pollut. Bull.*, 70? 2013? 81-89.
8. Suneel., V? Vethamony, P? Vinod Kumar, K? Babu, M. T? K. V. S. R. Prasad, 2013b. Simulation of Trajectories of Tar Ball Transport to the Goa Coast. *Water Air Soil Pollut*, 2013b, 24:1538, DOI 10.1007/s11270-013-1538-9.
9. Suneel. V., P. Vethamony., B. G. Naik., K. Vinod Kumar., L. Sreenu, S.V. Samiksha, Yunus Tai and K. Sudheesh. Source investigation of the tar balls deposited along the Gujarat coast, India using Chemical fingerprinting and transport modelling techniques. *Environmental Science and Technology*, DOI: 10.1021/es5032213.
10. Kvenvolden, A.K., F.D. Hostettler, P.R. Carlson, J.B. Rapp, C.N. Threlkeld and A. Warden., 1995. Ubiquitous tar balls with a California-surge signature on the shrelines of Prince William Sound, Alaska. *Environmenatal Science and Technolgy*, 2684-2694.
11. Wang, Z.D., Fingas, M., Sergy, G., 1995a. Chemical characterization of crude oil residues from an Arctic beach by GC/MS and GC/FID. *Environ. Sci. Technol.* 29 (10), 2622–2631.
12. Wang, Z.D., M. Fingas, M. Landriault, L. Sigouin, Y. Feng, and J. Mullin, 1997. Using systematic and comparative analytical data to identify the source of unknown oil on contaminated birds, *J. Chromatography*, 775, 251–265.
13. Wang, Z.D., M. Fingas, and L. Sigouin, 2001a. Characterization and identification of a “mystery” oil spill 146 *Oil Spill Environmental Forensics from Quebec (1999)*, *J. Chromatogr*, 909, 155–169.
14. Wang, Z.D., M. Fingas, and P. Lambert, 2004. Characterization and identification of Detroit River mystery oil spill (2002), *J. Chromatogr*, 1038, 201–214.
15. Wang, Z.D., M. Fingas, and D. Page, Oil spill identification, *J. Chromatogr.*, 1999a, 843, 369–411.
16. Stout, S.A., A.D. Uhler, K.J. McCarthy, and S. Emsbo-Mattingly, 2002. Chapter 6: Chemical fingerprinting of hydrocarbons, In: B.L. Murphy and R.D. Morrison (eds.), *Introduction to Environmental Forensics*, Academic Press, London, 139–260.
17. Daling, P.S., L.G. Faksness, A.B. Hansen, and S.A. Stout, 2002. Improved and standardized methodology for oil spill fingerprinting. *Environmental Forensics*, 3, 263–278.
18. Christensen, J.H., A.B. Hansen, J. Mortensen, G. Tomasi, and O. Andersen, 2004. Integrated methodology for forensic oil spill identification, *Environmental Science and Technology*, 38, 2912–2918
19. Peters, K.E., C.C. Walters, and J.W. Moldowan, 2005. *The Biomarker Guide (Two Volumes)*, 2nd Ed, Cambridge University Press, Cambridge, UK.
20. Barakat, A.O., Y. Qian, M. Kim, and M.C, 2002. Kennicutt II, Compositional changes of aromatic steroid hydrocarbons in naturally weathered oil residues in Egyptian Western Desert, *Environmental Forensics*, 3, 219–226
21. Barakat, A.O., Qion, Y., Kim, M., Kennicutt, M.C, 2001. Chemical characterization of naturally weathered oil residue in arid terrestrial environmental in Al-Alamein, Egypt. *Environmental Science and Technology* 27, 291–310.
22. Wang, Z., and Fingas, M., 2003. Development of oil hydrocarbon fingerprinting and identification techniques. *Marine Pollution Bulletin*, 47, 423–452.

23. Wang, Z., Fingas, M., Sergy, G. Study of 22-old Arrow oil samples using biomarker compounds by GC-MS, 1994b. *Environmental Science and Technology*, 28, 1733-1746.
24. Wang, Z.D., M. Fingas, and G. Sergy, 1995b. Chemical characterization of crude oil residues from an arctic beach by GC-MS and GC-FID. *Environmental Science and Technology*. 29, 2622– 2631.
25. Zakaria, M.P., A. Horinouchi., S. Tsutsumi., H. Takada., S. Tanabe., and A. Ismail., 2000. Oil pollution in the straits of Malacca, Malaysia: Application of Molecular Markers for source identification. *Environmental Science and Technology* 34, 1189-1196.
26. Zakaria, M. P., Tomoaki Okuda and Hideshige Takada., 2001. Polycyclic Aromatic Hydrocarbon (PAHs) and Hopanes in stranded Tar-balls on the coast of Peninsular Malaysia: Applications of Biomarkers for Identifying sources of oil pollution. *Marine Pollution Bulletin*. 42, 1357-1366.
27. Chandru, K., M.P. Zakaria, S. Anita, A. Shahbazi, M. Sakari, P.S. Bahry, C.R. Mohamed, 2008. Characterization of alkanes, hopanes, and polycyclic aromatic hydrocarbons (PAHs) in tar-balls collected from the East Coast of Peninsular Malaysia. *Marine Pollution Bulletin*, 56, 950-962
28. Rabbani, A.R., Galimov, E.M., 2000. Geochemical identification of oil source formations in southern Iran. *Geochemistry International* 38, 1198–1206.
29. Galimov, E.M., 1973. *Geochemistry of Carbon and its Applications in Oil and Gas Exploration*. Nedra Press, Moscow.
30. Galimov, E.M., Rabbani, A.R., 2001. Geochemical characteristics and origin of naturalgas in southern Iran. *Geochemistry International* 39, 780–792.
31. Rabbani, A.R., Kamali, M.R., 2005. Source rock evaluation and petroleum geochemistry, offshore SW Iran. *Journal of Petroleum Geology* 28, 413–428.
32. Jeffrey, A.W.A, 2006. Application of stable isotope ratios in spilled oil identification. In: Wang, Z., Stout, S.A. (Eds.), *Oil Spill Forensics: Fingerprinting and Source Identification*. Academic Press, NY, pp. 207–227
33. Macko, S.A., Parker, P.L., Botello, A. V., 1981. Persistence of spilled oil in a Texas salt marsh. *Environmental Pollution*, 2, 119-128.
34. Meckenstock, R. U.; Griebler, C.; Morasch, B.; Richnow, H. H. Stable isotope fractionation analysis as a tool to monitor biodegradation in contaminated aquifers. *J. Contam. Hydrol* 2004, 75, 215-255.
35. Mansuy, L., R. Paul Philip and John Allen., 1997. Source Identification of oil spills based on the isotopic composition of individual components in weathered oil samples. *Environmental Science and Technology*, 31, 3417-3425.
36. Li. Y and Yongqiang Xiong. 2009b. Identification and quantification of mixed sources of oil spills based on distributions and isotope profiles of long-chain n-alkanes. *Marine Pollution Bulletin* 58 (2009) 1868-1873.
37. Li, J.F., S. Fuller, J. Cattle, C.P. Way, and D.B. Hibbert, Matching fluorescence spectra of oil spills with spectra from suspect sources. *Analytica Chimica Acta*, 2004, 514(1), 51–56.
38. Betti, M., F. Boison, M. Eriksson, I. Tolosa., E. Vasileva, 2011. Isotope analysis for marine environmental studies. *International Journal of Mass Spectrometry*, 307(1-3), 192-199.
39. Oulhote, Y? B. Le Bot? S. Deguen, P. Glorennec., 2011. Using and interpreting isotope data for source identification. *Trends in Analytical Chemistry*, 30, 302-312.

40. Macko, S. A., Patrick, L. Parker, 1983. Strable Nitrogen and Carbon Isotope Ratios of Beach tar on South texas barrier Islands. *Marine Environmental Research*, 10, 93-103.
41. Murray, A.P., R.E. Summons, C.J. Boreham, and L.M. Dowling, 1994. Biomarker and n-alkane isotope profiles for Tertiary oils: Relationship to source rock depositional setting, *Organic Geochemistry*, 22, 521–542.
42. Kvenvolden, K.A., F.D. Hostettler, J.B. Rapp and P.R. Carlson, 1993. Hydrocarbons in oil residues on beaches of islands of Prince William Sound, Alaska, *Marine Pollution Bulletin*, 26, 24–29.
43. Wang, Z., M. Fingas, M. Landriault, L. Sigouin, B. Castle, D. Hostetter, D. Zhang, B. Spencer, 1998. Identification and linkage of tar balls from the coast of Vancouver Island and Northern California using GC-MS and Isotopic techniques. *Journal of High Resolution Chromatogram*, 21, 383-395.
44. Sosrowidjojo, I.B., Alexander, R. and Kagi, P., 1994. The biomarker composition of some crude oils from Sumatra. *Organic Geochemistry* 21, 303-312.
45. Mulabagal, V., F. Yin., G.F. John., J.S. Hayworth., T.P. Clement, 2010. Chemical fingerprinting of petroleum biomarkers in Deepwater Horizon oil spill samples collected from Alabama shoreline. *Marine Pollution Bulletin*, 70, 147–154.
46. Page, D. S., Boehm, P. D., Douglas, G. S., and Bence, A. E. "Identification of Hydrocarbon Sources in the Benthic Sediments of Prince William Sound and the Gulf of Alaska Following the Exxon Valdez Oil Spill," *Exxon Valdez Oil Spill: Fate and Effects in Alaskan Waters*, ASTM STP 1219, Peter G. Wells, James N. Butler, and Jane S. Hughes, Eds., American Society for Testing and Materials, Philadelphia, 1995.
47. Peters, K.E., Moldowan, J.M., 1991. Effects of source, thermal maturity, and biodegradation on the distribution and isomerization of homohopanes in petroleum. *Organic Geochemistry* 17, 47–61.
48. Peters, K.E., Moldowan, J.M., 1993. *The Biomarker Guide. Interpreting Molecular Fossils in Petroleum and Ancient Sediments*. Wiley, Prentice-Hall, EnglewoodCliffs, New Jersey.
49. Grantham, P.J., Wakefield, L.L., 1988. Variations in the sterane carbon number distributions of marine source rock derived crude oils through geological time. *Organic Geochemistry* 12, 61–73.
50. Shankar D., Vinayachandran P. N. and Unnikrishnan A. S. The monsoon currents in the north Indian Ocean, *Progressive Oceanography*, 2002, 52, 63– 120.

Supplementary Material



Fig. SM1. Tar ball deposit on the Mobor beach, Goa (26 May 2013)

SMI. Steranes Identification

The regular sterane compounds such as Cholestane (C_{27}), Ergostane (C_{28}), Stigmastane (C_{29}) and their S and R isomers are identified by performing the GC-MS run in m/z 217 window. The compounds were identified using the NIST reference library and Literature. The chromatograms for one crude (BHM) and one tar ball (CAN-1) samples are illustrated in the Fig. SM2, below.

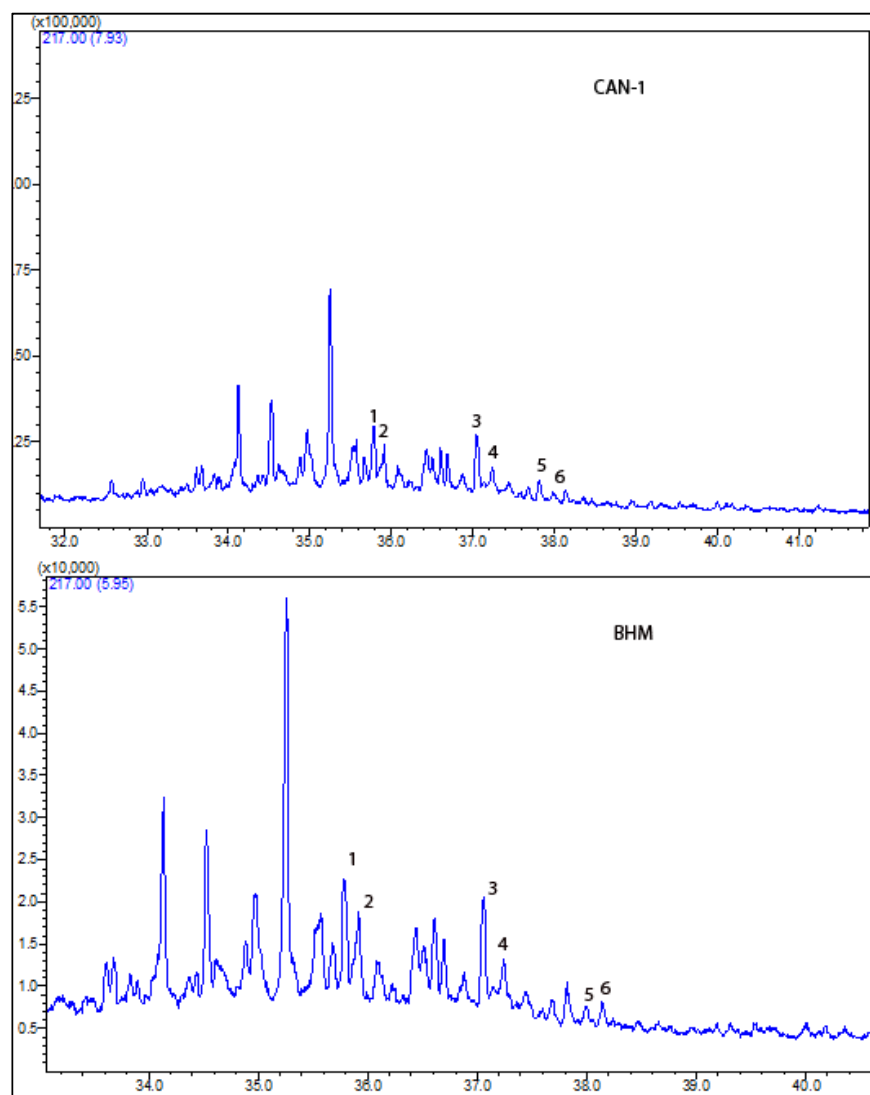


Fig. SM2. The regular Sterane compounds for CAN-1 tar ball and BHM crude oil samples. The peak numbers 1 to 6 are $5\alpha(\text{H}),14\beta(\text{H}),17\beta(\text{H})$ Cholestane-(C27 $\alpha\beta\beta\text{R}$), $5\alpha(\text{H}),14\beta(\text{H}),17\beta(\text{H})$ Cholestane-(C27 $\alpha\beta\beta\text{S}$), $5\alpha(\text{H}),14\beta(\text{H}),17\beta(\text{H})$ Ergostane-(C28 $\alpha\beta\beta\text{R}$), $5\alpha(\text{H}),14\beta(\text{H}),17\beta(\text{H})$ Ergostane-(C28 $\alpha\beta\beta\text{S}$), $5\alpha(\text{H}),14\beta(\text{H}),17\beta(\text{H})$ Stigmastane-(C29 $\alpha\beta\beta\text{R}$), $5\alpha(\text{H}),14\beta(\text{H}),17\beta(\text{H})$ Stigmastane-(C27 $\alpha\beta\beta\text{S}$) respectively.

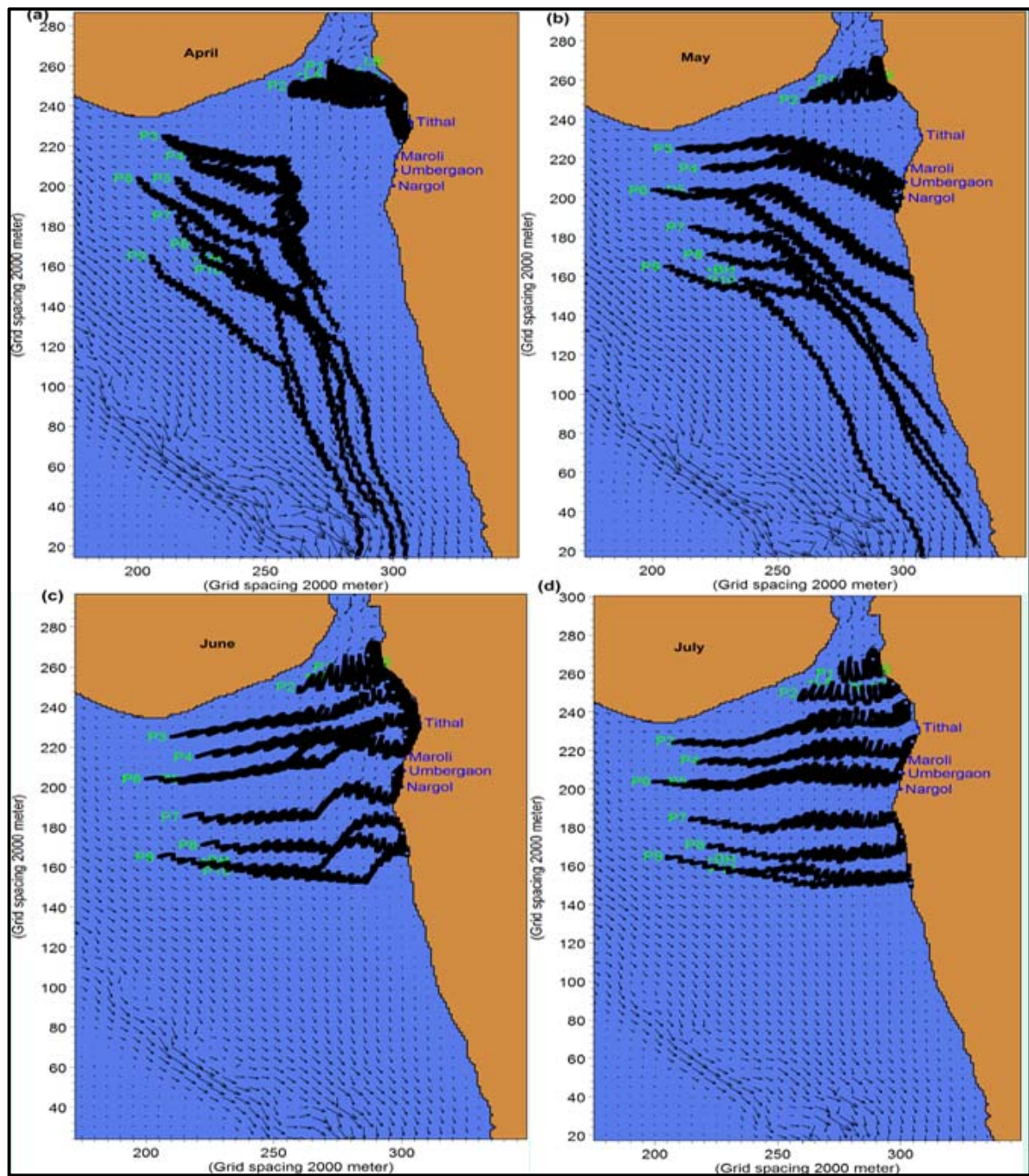


Fig. SM3. Particle trajectories for April, May, June and July 2012 taken from Suneel et al. 2014

Tables

Table. SM 1. Acronyms used in the study

Acronym	Expansion
CSIA	Compound Specific Isotope Analysis
PCA	Principle Component Analysis
WCI	West Coast of India
BH	Bombay High
BHM	Bombay High Mut
BHH	Bombay High Hut
CRN	CAIRN oil fields
NIK	NIKO oil fields
MSC	MSC Chitra tanker spill
DRs	Diagnostic Ratios
GC-FID	Gas Chromatograph-Flame Ionization Detector
GC-MS	Gas Chromatograph-Mass Spectrometer
GC-IRMS	Gas Chromatograph-Isotope Ratio Mass Spectrometer
AS	Arabian Sea
PAH	Polycyclic Aromatic Hydrocarbons
DCM	Dichloromethane
EPA	Environment Protection Agency
CPI	Carbon Preference Index
Pr/Py	The ratio of Pristane to Phytane
L/H	Ratio of sum of low molecular to sum of high molecular n-alkanes [$\sum(n-C_{16} \text{ to } n-C_{26}) / \sum(n-C_{27} \text{ to } n-C_{36})$]
WI	Weathering Index
MECO	Middle East Crude Oil
SEACO	South East Asia Crude Oil

Table SM2. Sampling type and details.

code	Coordinates	Type	Place of collection	Date	Buoyancy	Sand (%)
CAN-1_{tb}	15°30'51.08"N 73°45'49.33"E	Tar ball	Candolim beach	27/05/2013	floating	
CAN-2_{tb}	15°30'53.26"N 73°45'48.69"E	Tar ball	Candolim beach	27/05/2013	floating	n.m
VAG-1_{tb}	15°36'05.78"N 73°44'02.15"E	Tar ball	Vagator beach	27/05/2013	floating	
VAG-2_{tb}	15°36'09.71"N 73°44'01.16"E	Tar ball	Vagator beach	27/05/2013	floating	n.m
AGO-1_{tb}	15°02'36.24"N 73°59'09.73"E	Tar ball	Agonda beach	28/05/2013	floating	
AGO-2_{tb}	15°02'28.75"N 73°59'12.72"E	Tar ball	Agonda beach	28/05/2013	floating	20.22
COL-1_{tb}	15°16'29.76"N 73°54'48.46"E	Tar ball	Colva beach	28/05/2013	floating	
COL-2_{tb}	15°16'23.30"N 73°54'50.67"E	Tar ball	Colva beach	28/05/2013	floating	22.86
BEN-1_{tb}	15°15'00.90"N 73°55'15.05"E	Tar ball	Benaulim beach	28/05/2013	floating	
BEN-2_{tb}	15°14'55.30"N 73°55'16.57"E	Tar ball	Benaulim beach	28/05/2013	floating	22.29
VEL-1_{tb}	15°21'04.60"N 73°53'08.22"E	Tar ball	Velsao beach	28/05/2013	floating	
VEL-2_{tb}	15°20'59.29"N 73°53'10.57"E	Tar ball	Velsao beach	28/05/2013	floating	16.68
VAR-1_{tb}	15°13'42.35"N 73°55'37.94"E	Tar ball	Varca beach	28/05/2013	floating	
VAR-2_{tb}	15°13'38.23"N 73°55'37.89"E	Tar ball	Varca beach	28/05/2013	floating	n.m
MAJ-1_{tb}	15°18'46.21"N 73°54'03.62"E	Tar ball	Majorda beach	28/05/2013	floating	
MAJ-2_{tb}	15°18'37.20"N 73°54'06.75"E	Tar ball	Majorda beach	28/05/2013	floating	17.32
MOB-1_{tb}	15°09'21.00"N 73°56'44.44"E	Tar ball	Mobor beach	28/05/2013	floating	
MOB-2_{tb}	15°09'17.71"N 73°56'44.95"E	Tar ball	Mobor beach	28/05/2013	floating	n.m
BHM_{oil}	19.41°N 71.33° E	Crude oil	Uran plant, Mumbai	24/06/2013	floating	nd
BHH_{oil}	19.41°N 71.33° E	Crude oil	Uran plant, Mumbai	24/06/2013	floating	nd
CRN_{oil}	21°1'55"N 72°33'17"E	Crude oil	Cairn (pvt) Ltd, Surat	24/06/2013	floating	nd
NIK_{oil}	21°03'41.88"N 72°36'57.17"E	Crude oil	Niko (pvt) Ltd, Surat	24/06/2013	floating	nd
MSC_{oil}	18.9051°N 72.8760°E	Spilled oil	off Mumbai	09/08/2010	floating	nd

Nd-not detected, n.m-not measured

Table SM3. The DRs of n-alkanes for the tar ball samples and crude oils

Sample	Pr/Ph	nC ₁₇ /Pr	nC ₁₈ /Ph	nC ₁₇ /nC ₁₈	CPI	L/H	WI
AGO-1	4.6	1.01	4.95	0.94	1.1	1.04	0.05
AGO-2	4.59	1	4.86	0.94	1.09	0.78	0.05
CAN-1	4.13	0.98	5.07	0.79	1.1	0.85	0.01
CAN-2	4.04	0.98	4.91	0.81	1.1	0.92	0.01
MOB-1	3.29	0.98	4.65	0.69	1.11	0.74	0.004
MOB-2	4.13	1	5.02	0.82	1.09	1.13	0.01
VAR-1	4.75	0.97	5.04	0.92	1.11	0.82	0.04
VAR-2	4.31	0.92	4.52	0.88	1.1	0.81	0.04
VAG-1	4.08	0.99	5.03	0.8	1.1	0.95	0.01
VAG-2	4.27	0.99	5.09	0.83	1.09	0.84	0.02
BEN-1	4.72	0.99	5.01	0.94	1.1	0.75	0.06
BEN-2	4.44	0.99	4.93	0.89	1.09	0.79	0.04
MAJ-1	4.3	1.01	4.79	0.91	1.1	0.92	0.05
MAJ-2	4.76	0.97	5.02	0.92	1.1	0.69	0.05
VEL-1	4.64	0.35	2.13	0.77	1.11	0.35	0.01
VEL-2	3.28	0.97	4.78	0.67	1.1	0.89	0.002
COL-1	4.77	1	5.05	0.94	1.1	1.09	0.08
COL-2	4.39	1.06	4.92	0.95	1.09	0.9	0.07
BHM	4.99	0.96	4.81	1	1.09	1.53	0.26
BHH	6.03	0.94	5.67	1	1.11	1.37	0.21
CRN	6.38	1.71	9.83	1.11	1.1	3.1	0.73
NIK	5.56	1.78	9.85	1	1.1	1.77	0.29
MSC	0.73	5.97	4.1	1.07	1.1	3.03	1.07

Table SM4. Diagnostic Ratios of Pentacyclic triterpanes for tar ball samples and crude oils

Samples	C_{29}/C_{30}	$\sum C_{31-35}/C_{30}$	Tm/C_{30}	Oleanane/ C_{30}	Ts/Tm	$C_{31}S/(S+R)$	$C_{32}S/(S+R)$	$C_{33}S/(S+R)$	$C_{34}S/(S+R)$	$C_{35}S/(S+R)$
AGO-1 _{tb}	0.59	1.28	0.02	0.41	5.35	0.10	0.48	0.33	0.56	0.67
AGO-2 _{tb}	0.53	1.68	0.21	0.40	0.60	0.11	0.45	0.25	0.49	0.25
CAN-1 _{tb}	0.56	1.60	0.22	0.39	0.55	0.10	0.49	0.27	0.22	0.33
CAN-2 _{tb}	0.56	1.57	0.22	0.40	0.49	0.10	0.49	0.27	0.26	0.31
MOB-1 _{tb}	0.58	1.61	0.20	0.39	0.62	0.10	0.48	0.24	0.21	0.32
MOB-2 _{tb}	0.59	1.28	0.22	0.40	0.57	0.10	0.50	0.33	0.37	0.53
VAR-1 _{tb}	0.56	1.40	0.20	0.39	0.58	0.10	0.52	0.34	0.25	0.33
VAR-2 _{tb}	0.56	1.41	0.22	0.41	0.55	0.10	0.49	0.33	0.17	0.48
VAG-1 _{tb}	0.58	1.58	0.22	0.40	0.59	0.09	0.48	0.33	0.19	0.38
VAG-2 _{tb}	0.59	1.37	0.21	0.40	0.57	0.10	0.48	0.34	0.33	0.47
BEN-1 _{tb}	0.52	1.24	0.21	0.39	0.58	0.09	0.49	0.34	0.59	0.61
BEN-2 _{tb}	0.55	1.58	0.21	0.40	0.60	0.10	0.49	0.26	0.20	0.25
MAJ-1 _{tb}	0.56	1.44	0.20	0.38	0.56	0.11	0.49	0.34	0.23	0.35
MAJ-2 _{tb}	0.60	1.37	0.21	0.42	0.59	0.09	0.44	0.30	0.48	1.0
VEL-1 _{tb}	0.55	1.37	0.22	0.41	0.59	0.10	0.48	0.33	0.34	0.46
VEL-2 _{tb}	0.59	1.27	0.21	0.40	0.56	0.10	0.48	0.33	0.54	0.67
COL-1 _{tb}	0.55	1.32	0.21	0.40	0.60	0.10	0.48	0.33	0.53	0.65
COL-2 _{tb}	0.57	1.46	0.21	0.40	0.57	0.10	0.48	0.34	0.19	0.3
BHM _{oil}	0.57	1.21	0.22	0.36	0.54	0.09	0.47	0.33	0.44	1
BHH _{oil}	0.56	1.40	0.24	0.18	0.34	0.05	0.47	0.35	0.45	0.65
CRN _{oil}	0.52	0.90	0.16	0.11	0.64	0.05	0.49	0.29	0.60	0.57
NIK _{oil}	0.52	0.98	0.18	0.11	0.56	0.07	0.45	0.31	0.36	0.42
MSC _{oil}	0.97	2.94	0.31	0.09	0.66	-	0.55	0.62	0.57	0.54